

Cationic Mn<sub>4</sub> Single-Molecule Magnet with a Sterically Isolated CoreKatie J. Heroux,<sup>†</sup> Hajrah M. Quddusi,<sup>‡</sup> Junjie Liu,<sup>§</sup> James R. O'Brien,<sup>||</sup> Motohiro Nakano,<sup>⊥</sup> Enrique del Barco,<sup>‡</sup> Stephen Hill,<sup>||</sup> and David N. Hendrickson<sup>\*,†</sup><sup>†</sup>Department of Chemistry and Biochemistry, University of California at San Diego, La Jolla, California 92093, United States<sup>‡</sup>Department of Physics, University of Central Florida, Orlando, Florida 32816, United States<sup>§</sup>Department of Physics, University of Florida, Gainesville, Florida 32611, United States<sup>||</sup>Quantum Design, San Diego, California 92121, United States<sup>⊥</sup>Division of Applied Chemistry, Osaka University, Suita, Osaka 565-0871, Japan<sup>\*</sup>National High Magnetic Field Laboratory and Department of Physics, Florida State University, Tallahassee, Florida 32310, United States

## S Supporting Information

**ABSTRACT:** The synthesis, structure, and magnetic properties of a ligand-modified Mn<sub>4</sub> dicubane single-molecule magnet (SMM), [Mn<sub>4</sub>(Bet)<sub>4</sub>(mdea)<sub>2</sub>(mdeaH)<sub>2</sub>](BPh<sub>4</sub>)<sub>4</sub>, are presented, where the cationic SMM units are significantly separated from neighboring molecules in the crystal lattice. There are no cocrystallized solvate molecules, making it an ideal candidate for single-crystal magnetization hysteresis and high-frequency electron paramagnetic resonance studies. Increased control over intermolecular interactions in such materials is a crucial factor in the future application of SMMs.

Since the discovery of single-molecule magnets (SMMs) in 1993,<sup>1</sup> much research has focused on tailoring these single-domain magnetic molecules for applications in high-density information storage and quantum information processing.<sup>2</sup> The quantum phenomena exhibited by SMMs, however, are extremely sensitive to environmental couplings. Interactions between neighboring SMMs in the crystal lattice (through-space and through-bond) can be detrimental to the magnetic and quantum properties of SMMs.<sup>2b</sup> Thus, the goal of this research was to synthesize cationic SMMs with limited intermolecular interactions through isolation with bulky organic counteranions.

Glycine betaine (O<sub>2</sub>CCH<sub>2</sub>NMe<sub>3</sub>) is a zwitterionic compound. The first Mn<sub>12</sub>-acetate SMM functionalized with betaine ligands was the polycationic cluster [Mn<sub>12</sub>O<sub>12</sub>(Bet)<sub>16</sub>(EtOH)<sub>4</sub>](PF<sub>6</sub>)<sub>14</sub>·4 MeCN·H<sub>2</sub>O,<sup>3</sup> which was prepared for self-assembly on soft media or for deposition of monolayers onto anionic metal surfaces.<sup>3,4</sup> However, because larger SMMs are often subject to solvent and crystal disorder, we have chosen here to employ this strategy on the small Mn<sub>4</sub> dicubane SMMs,<sup>5</sup> which are highly amenable to ligand modification and have well-defined structural and magnetic properties.

The reaction of Mn(NO<sub>3</sub>)<sub>2</sub>·4H<sub>2</sub>O, BetHBPPh<sub>4</sub>, mdeaH<sub>2</sub>, and NEt<sub>3</sub> in MeOH or MeCN followed by slow vapor diffusion (Et<sub>2</sub>O or *i*Pr<sub>2</sub>O) affords X-ray-quality crystals of [Mn<sub>4</sub>(Bet)<sub>4</sub>(mdea)<sub>2</sub>(mdeaH)<sub>2</sub>](BPh<sub>4</sub>)<sub>4</sub>, henceforth Mn<sub>4</sub>-Bet, where Bet is glycine betaine and mdeaH<sub>2</sub> is *N*-methyldiethanolamine. The centrosymmetric Mn<sub>4</sub>-Bet (ORTEP in Figure 1) crystallizes in

the triclinic  $P\bar{1}$  space group with half of the molecule in the asymmetric unit. The [Mn<sub>2</sub><sup>II</sup>Mn<sub>2</sub><sup>III</sup>O<sub>6</sub>]<sup>4+</sup> core resembles two face-sharing cubanes missing opposite vertices with two heptacoordinate Mn<sup>II</sup> ions (Mn1) in the “wing” positions and two hexacoordinate Mn<sup>III</sup> ions (Mn2) in the “body” positions. This pseudodicubane core is isostructural with the previously reported Mn<sub>4</sub>-benzoate dicubanes [Mn<sub>4</sub>(O<sub>2</sub>CPh)<sub>4</sub>(mdeaH)<sub>2</sub>(mdea)<sub>2</sub>] reported by Foguet-Albiol et al.<sup>5b</sup> and [Mn<sub>4</sub>(O<sub>2</sub>CPh)<sub>4</sub>(bdea-H)<sub>2</sub>(bdea)<sub>2</sub>] reported by Ako et al.<sup>5c</sup>

A stereoplot of the unit cell of Mn<sub>4</sub>-Bet is shown in Figure S1 (in the Supporting Information, SI), emphasizing the increased steric isolation provided by the BPh<sub>4</sub><sup>-</sup> anions. The molecule packs in 2D sheets in the crystallographic *ab* plane with closest intermolecular Mn···Mn distances of ~10 Å within each layer and nearly 15 Å between layers. This separation between neighboring molecules is significantly increased from the benzoate analogues whose shortest intermolecular Mn···Mn distances are only 8–9 Å. The increased steric isolation of a single Mn<sub>4</sub>-Bet molecule can most clearly be seen in the space-filling model shown in Figure 2. This is expected to lead to a significant decrease in intermolecular through-bond magnetic exchange and a more moderate decrease in through-space dipolar interactions.

Direct-current (dc) magnetic susceptibility data collected in applied fields of 1–5 T, and in the temperature range from 300 to 1.8 K, are shown in Figure 3. A full-matrix diagonalization approach was employed in order to fit the dc data to a multispin Hamiltonian including isotropic exchange, axial (*d*) and rhombic (*e*) zero-field-splitting (zfs) terms, and a Zeeman interaction (see the SI). The resulting fits are shown as solid black curves in Figure 3 (the zero-field eigenvalue spectrum is shown in Figure S3 in the SI), which gave a spin *S* = 9 ground state with *g* = 1.81(1), *J*<sub>bb</sub> = 7.6(8) K, *J*<sub>wb1</sub> = 5.8(1) K, and *J*<sub>wb2</sub> = -1.0(1) K and single-ion zfs parameters of *d* = -5.9(2) K and *e* = 0.8(2) K for Mn<sup>III</sup>; the zfs for Mn<sup>II</sup> was assumed to be negligible in comparison.

For an experimental determination of the energy barrier to magnetization relaxation resulting from the appreciable easy-axis anisotropy, the alternating-current (ac) magnetic susceptibility of Mn<sub>4</sub>-Bet was measured. Data were collected in the temperature

Received: May 13, 2011

Published: July 13, 2011

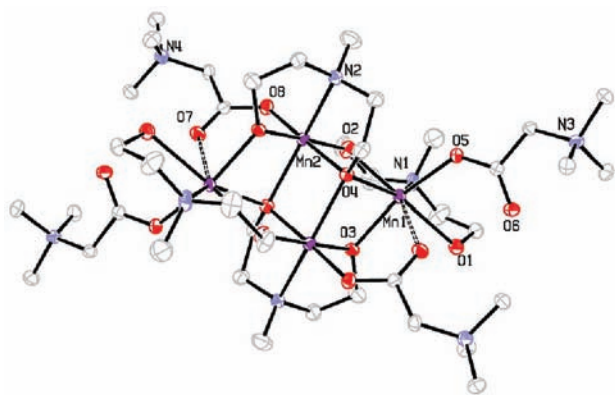


**Figure 1.** ORTEP of  $\text{Mn}_4\text{-Bet}$  with  $\text{BPh}_4^-$  anions and H atoms omitted for clarity and thermal ellipsoids drawn at the 30% probability level.

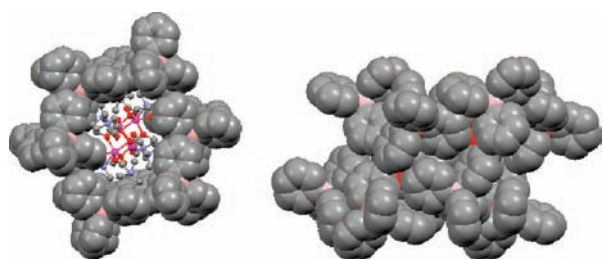


**Figure 2.** Space-filling model of  $\text{BPh}_4^-$  anions encapsulating a single  $\text{Mn}_4\text{-Bet}$  unit in the crystal packing of  $\text{Mn}_4\text{-Bet}$ .

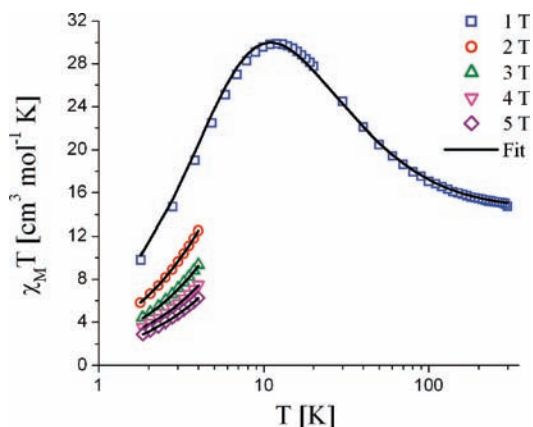


**Figure 3.** dc magnetic susceptibility for  $\text{Mn}_4\text{-Bet}$  with theoretical fits (by full-matrix diagonalization) represented by solid black curves.

range from 6 to 1.8 K and at frequencies from 0.1 to 10 kHz, as shown in Figure S4 in the SI. A frequency-dependent out-of-phase signal is observed below 5.2 K, indicating a sizable barrier. An Arrhenius plot (Figure S4 in the SI) of the out-of-phase peak positions gives a value of  $E_a = 20.5$  K, which agrees remarkably well with high-frequency electron paramagnetic resonance (HFEP) and magnetization hysteresis measurements (vide infra).

$\text{Mn}_4\text{-Bet}$  is an ideal candidate for high-resolution single-crystal magnetization hysteresis and HFEP studies in that it possesses no cocrystallized solvate molecules, thereby eliminating a major source of disorder.<sup>6</sup> In addition, there is no apparent disorder associated with the ligands and only one molecule per unit cell, i.e.,

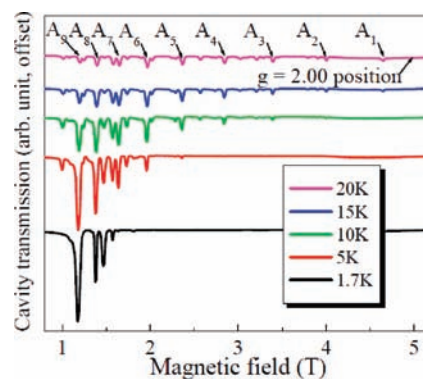


**Figure 4.** Temperature-dependent HFEP spectra measured with the field applied parallel to the easy axis at a frequency of 139.5 GHz.

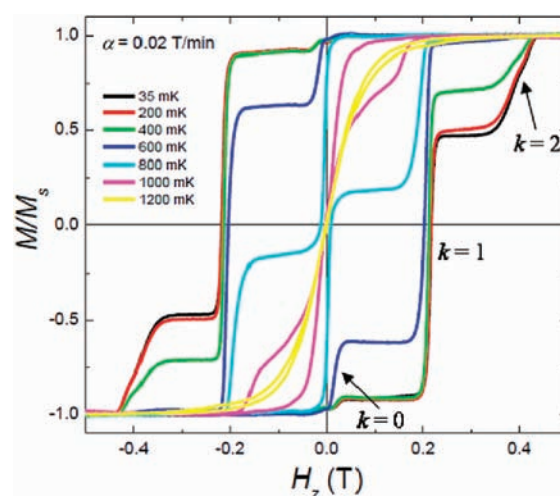


**Figure 5.** Temperature-dependent magnetization hysteresis for  $\text{Mn}_4\text{-Bet}$ .

only one molecular orientation (Figure S5 in the SI). In order to more precisely characterize the low-energy spectrum of  $\text{Mn}_4\text{-Bet}$ , temperature-dependent (1.7–20 K) HFEP measurements were performed. Figure 4 displays spectra obtained for a single crystal with the magnetic field applied within a few degrees of the easy axis. Multiple series of resonances (sharp dips in transmission) are observed at elevated temperatures, indicating the presence of many low-lying excited spin states ( $S < 9$ ). However, careful inspection reveals a dominant series of nine peaks (labeled  $A_1$ – $A_9$ ) that can be identified with the  $S = 9$  ground state on the basis of their relative spacing and temperature dependence.<sup>7,8</sup> For this orientation, the lowest-field resonance ( $A_9$ ) corresponds to the  $m_S = -9$  to  $-8$  transition. On the basis of the shift in the spectral weight to lower fields (specifically to  $A_9$ ) upon a decrease in the temperature, one can deduce that molecular anisotropy is of the easy-axis type ( $D < 0$ ),<sup>9</sup> as required for a SMM. This is further corroborated via measurements made with the field in the hard plane (Figure S6 in the SI), which display the opposite trend.

To determine if  $\text{Mn}_4\text{-Bet}$  exhibits magnetic bistability/hysteresis and quantum tunneling of magnetization (QTM), temperature-dependent magnetization ( $M/M_s$ ) versus longitudinal field ( $H_z$ ) data were collected for a single crystal in the temperature range from 35 to 1200 mK.<sup>8</sup> Hysteresis is indeed observed for  $\text{Mn}_4\text{-Bet}$ , as shown in Figure 5. The data also clearly reveal sharp, evenly spaced vertical steps in the hysteresis loops, indicative of QTM.

The hysteresis is essentially temperature-independent below  $\sim 300$  mK, where pure ground-state tunneling sets in. Thermally assisted tunneling is seen as the temperature is increased until the blocking temperature of  $\sim 1.2$  K is reached, at which point the hysteresis loop collapses.

The vertical steps in the hysteresis plots at  $H_z = 0, 0.2,$  and  $0.4$  T can be assigned to QTM transitions between  $m_S = -9$  and  $9 - k$  states, where  $k = 0, 1,$  and  $2,$  respectively. These QTM resonances occur at a regular interval of  $0.2$  T ( $\Delta H$ ), as shown in the first derivative plot of the hysteresis loops in Figure S7 in the SI. There is a small shift of  $\sim 0.02$  T for all resonances as well as some other minor peaks (mostly in the  $k = 2$  resonance and at higher temperatures), which are likely due to dipolar effects. The molecular zfs parameter,  $D$ , associated with the  $S = 9$  ground state was calculated to be  $-0.258$  K from the equation  $\Delta H = k|D|/g\mu_0\mu_B$ . This value is in excellent agreement with the activation barrier ( $E_a = |DS^2|$ ) estimated from ac susceptibility measurements.

A multispin Hamiltonian was employed to simulate the combined HFEPR and hysteresis data sets via exact matrix diagonalization (see the SI). A single set of parameters was found to give good overall agreement with both sets of measurements, including the transverse-field quenching of QTM (Berry phase interference).<sup>8</sup> The resulting simulations of both the easy-axis and hard-plane HFEPR data are displayed in Figure S8 in the SI. The parameters employed for these simulations are  $g = 2.00,$   $J_{bb} = 1.68$  K,  $J_{wb1} = 1.92$  K, and  $J_{wb2} = 0.60$  K; single-ion zfs parameters  $d = -4.99$  K and  $e = 0.82$  K for  $Mn^{III}$  and  $d = -0.67$  K and  $e = 0$  for  $Mn^{II}$ ; a dipolar interaction was also included (see the SI). We note that zfs on the  $Mn^{II}$  sites proved to be essential in order to account for all aspects of the HFEPR and hysteresis measurements.<sup>8</sup> The relatively weak exchange within the cluster is consistent with the observation of significant HFEPR intensity due to low-lying spin states.

In summary, a new cationic  $S = 9$   $Mn_4$  dicubane SMM has been synthesized with enhanced steric isolation of the magnetic core due to bulky  $BPh_4^-$  anions. The subsequent reduction of intermolecular exchange interactions leads to increased electronic isolation of the ground state. The high crystal quality and single orientation of this molecule in the unit cell made  $Mn_4$ -Bet an ideal complex for single-crystal measurements.  $Mn_4$ -Bet exhibits some of the sharpest HFEPR spectra observed for a SMM. Furthermore, magnetization hysteresis loops show well-defined QTM resonances, a signature characteristic of SMMs. This molecule has been shown to exhibit other quantum mechanical phenomena such as quantum spin phase (or Berry phase) interference, as well as other unique properties experimentally observed for the first time, the details of which are communicated in a separate publication.<sup>8</sup>

## ASSOCIATED CONTENT

**S Supporting Information.** X-ray crystallographic data in CIF format, experimental and crystallographic details, magnetic susceptibility, and EPR fitting models. This material is available free of charge via the Internet at <http://pubs.acs.org>. The CIF file for  $Mn_4$ -Bet (CCDC 790437) has also been deposited with the Cambridge Crystallographic Data Centre. These data can be obtained free of charge from the Cambridge Crystallographic Data Centre via [www.ccdc.cam.ac.uk/data\\_request/cif](http://www.ccdc.cam.ac.uk/data_request/cif).

## AUTHOR INFORMATION

### Corresponding Author

\*E-mail: [dhendrickson@ucsd.edu](mailto:dhendrickson@ucsd.edu). Fax: +858-534-5383.

## ACKNOWLEDGMENT

The authors acknowledge support from NSF, specifically from Grants CHE-0714488 (to K.J.H. and D.N.H.), DMR-0747587 (to H.M.Q. and E.d.B.), and DMR-0804408 (to J.L. and S.H.).

## REFERENCES

- (1) (a) Sessoli, R.; Tsai, H. L.; Schake, A. R.; Wang, S. Y.; Vincent, J. B.; Foltling, K.; Gatteschi, D.; Christou, G.; Hendrickson, D. N. *J. Am. Chem. Soc.* **1993**, *115*, 1804–1816. (b) Sessoli, R.; Gatteschi, D.; Caneschi, A.; Novak, M. A. *Nature* **1993**, *365*, 141–143.
- (2) (a) Stamp, P. C. E.; Gaita-Arino, A. *J. Mater. Chem.* **2009**, *19*, 1718–1730. (b) Dube, M.; Stamp, P. C. E. *Chem. Phys.* **2001**, *268*, 257–272. (c) Leuenberger, M. N.; Loss, D. *Phys. Rev. B* **2000**, *61*, 12200–12203.
- (3) Coronado, E.; Feliz, M.; Forment-Aliaga, A.; Gomez-Garcia, C. J.; Llusar, R.; Romero, F. M. *Inorg. Chem.* **2001**, *40*, 6084.
- (4) Forment-Aliaga, A.; Coronado, E.; Feliz, M.; Gaita-Arino, A.; Llusar, R.; Romero, F. M. *Inorg. Chem.* **2003**, *42*, 8019–8027.
- (5) (a) Beedle, C. C.; Heroux, K. J.; Nakano, M.; DiPasquale, A. G.; Rheingold, A. L.; Hendrickson, D. N. *Polyhedron* **2007**, *26*, 2200–2206. (b) Foguet-Albiol, D.; O'Brien, T. A.; Wernsdorfer, W.; Moulton, B.; Zaworotko, M. J.; Abboud, K. A.; Christou, G. *Angew. Chem., Int. Ed.* **2005**, *44*, 897–901. (c) Ako, A. M.; Mereacre, V.; Hewitt, I. J.; Clerac, R.; Lecren, L.; Anson, C. E.; Powell, A. K. *J. Mater. Chem.* **2006**, *16*, 2579–2586. (d) Beedle, C. C.; Stephenson, C. J.; Heroux, K. J.; Wernsdorfer, W.; Hendrickson, D. N. *Inorg. Chem.* **2008**, *47* (23), 10798–10800. (e) Brechin, E. K.; Yoo, J.; Nakano, M.; Huffman, J. C.; Hendrickson, D. N.; Christou, G. *Chem. Commun.* **1999**, 783–784. (f) Yoo, J.; Brechin, E. K.; Yamaguchi, A.; Nakano, M.; Huffman, J. C.; Maniero, A. L.; Brunel, L. C.; Awaga, K.; Ishimoto, H.; Christou, G.; Hendrickson, D. N. *Inorg. Chem.* **2000**, *39*, 3615–3623. (g) Yang, E. C.; Harden, N.; Wernsdorfer, W.; Zakharov, L.; Brechin, E. K.; Rheingold, A. L.; Christou, G.; Hendrickson, D. N. *Polyhedron* **2003**, *22*, 1857–1863. (h) Wittick, L. M.; Murray, K. S.; Moubarak, B.; Batten, S. R.; Spiccia, L.; Berry, K. J. *Dalton Trans.* **2004**, 1003–1011.
- (6) Lawrence, J.; Yang, E.-C.; Edwards, R.; Olmstead, M. M.; Ramsey, C.; Dalal, N. S.; Gantzel, P. K.; Hill, S.; Hendrickson, D. N. *Inorg. Chem.* **2008**, *47*, 1965–1974.
- (7) Liu, J.; Beedle, C. C.; Quddusi, H. M.; del Barco, E.; Hendrickson, D. N.; Hill, S. *Polyhedron* **2011**, doi:10.1016/j.poly.2011.01.029
- (8) Quddusi, H. M.; Liu, J.; Singh, S.; Heroux, K. J.; del Barco, E.; Hill, S.; Hendrickson, D. N. *Phys. Rev. Lett.* **2011**, *106*, 227201.
- (9) (a) Rumberger, E. M.; Hill, S.; Edwards, R. S.; Wernsdorfer, W.; Zakharov, L. N.; Rheingold, A. L.; Christou, G.; Hendrickson, D. N. *Polyhedron* **2003**, *22*, 1865–1870. (b) Collison, D.; Murrie, M.; Oganessian, V. S.; Piligkos, S.; Poolton, N. R. J.; Rajaraman, G.; Smith, G. M.; Thomson, A. J.; Timko, G. A.; Wernsdorfer, W.; Winpenny, R. E. P.; McInnes, E. J. L. *Inorg. Chem.* **2003**, *42*, 5293–5303. (c) McInnes, E. J. L.; Piligkos, S.; Timco, G. A.; Winpenny, R. E. P. *Coord. Chem. Rev.* **2005**, *249*, 2577–2590.